Energy, Mines and Resources Canada | Énergie, Mines et Ressources Canada

CANMET

Canada Centre for Mineral and Energy Technology | Centre canadien de la technologie des minéraux et de l'énergie

ELECTRON MICROPROBE STUDIES ON CO[illegible]ON INHIBITOR FILMS

R.H. Packwood, V.E. Moore, V.S. Sastri and J. Bednar
Engineering & Metal Physics
and Corrosion Science Sections

March 1984

This document is [illegible]
[illegible]
(CANMET)
[illegible]

17 pp

MICROMEDIA

MINERALS RESEARCH PROGRAM
PHYSICAL METALLURGY RESEARCH LABORATORIES
REPORT MRP/PMRL 84-9(TR)

PHYSICAL METALLURGY RESEARCH LABORATORIES
REPORT MRP/PMRL 84-9(TR)

ELECTRON MICROPROBE STUDIES ON CORROSION INHIBITOR FILMS

by

R.H. Packwood*, V.E. Moore**, V.S. Sastri*** and J. Bednar****

ABSTRACT

This work shows that, in certain circumstances, the electron microprobe is capable of detecting and measuring monolayers and fractions of monolayers of surface deposits.

---

*Research scientist, **Technologist, Engineering & Metal Physics Section, *** Research scientist, ****Technologist, Corrosion Science Section, Physical Metallurgy Research Laboratories, CANMET, Energy, Mines and Resources Canada, Ottawa

LABORATOIRE DE RECHERCHE EN MÉTALLURGIE PHYSIQUE
RAPPORT PRM/LRMP 84-9(TR)

ETUDE PAR MICRASONDE DES FILMS ANTICORROSIFS

par

R.H. Packwood*, V.E. Moore**, V.S. Sastri*** et J. Bednar****

RÉSUMÉ

Ce travail indique que sous certaines conditions, le microanalyseur à sonde électronique peut détecter et mesurer les couches atomiques, ainsi que des fractions de couches atomiques des dépôts superficiels.

---

*Chercheurs scientifiques, **Technologist, Engineering & Metal Physics Section, *** Chercheurs scientifiques, ****Technologist, Corrosion Science Section, Laboratoires de Recherche en Métallurgie Physique, CANMET, Énergie, Mines et Ressources Canada, Ottawa

INTRODUCTION

The electron microprobe is not a surface sensitive instrument, at least, not in the modern meaning of the terms, i.e., sensing only the outermost 0.01-10 atomic layers of a sample. The X-ray signal in a probe is generated in the outer 0.05-2 μm of a sample at a depth which depends upon the sample's average atomic number and the accelerating potential of the electron beam. However, X-ray signals from pure materials are very large even for a few nA of current, a typical count rate being 10^4 c/s, with a peak to background ratio of over 1000:1. Hence, it is comparatively simple to detect one part in 10^3 or 10^4 of a substance. Noting that the signal is generated in the first ~5000 atomic layers it is simply a matter of physics to calculate the signal to be expected from a single monolayer of material and by extension the signal from fractions of monolayers. It transpires that signals, of the order of 10-100 c/s may be expected from a monolayer of average atomic number at 10 kV accelerating potential.

There is a caveat on this statement - a monolayer on a solid support has to be <u>different from the support in a significant manner</u> for it to be detectable above the much stronger background X-ray signal (count rate) generated by the massive solid support. For example, a layer of iron oxide on iron would not be detectable as iron oxide, but as an oxygen signal, and the presence of iron oxide would have to be inferred from other considerations. At first sight, this appears to be a severe limitation on using the microprobe for surface investigations. Indeed, it would be, but for one fact: many surface films of interest are distinctly different from the solid substrate on which they are present. Vacuum sputtered layers used in optics, and microelectronic circuits often fall into this category.

Another instance where thin films play an important role is in corrosion inhibition. Here, small quantities of corrosion inhibitors are added to closed cooling systems such as in automobiles, to prevent the formation of rust. Larger examples are to be found in chemical plants, oil wells and coal slurry pipelines where the inhibitor species is invariably sufficiently different chemically from the material to be protected that its presence can be readily detected.

A second point to emphasize is that for "real-life" samples, the lack of extreme surface specificity of the microprobe can be an advantage. A thin

deposit or film on a surface may be covered by contaminant films consisting of moisture or finger print residues, oil and the like. Provided that the contamination is not gross, the electron beam can pass through it and generate X-rays in the film of interest; in turn the X-rays can readily escape the outer contaminant layer and be counted by the spectrometer. This is in distinct contrast to the ESCA/Auger techniques which require the complete removal of contaminant layers by ion milling, before the primary or secondary electrons that constitute the signal can escape from the layer of interest. The chances of losing or modifying a thin layer are quite large during the ion sputtering process.

With the above considerations in mind, a microprobe investigation of inhibitor films on mild steel samples was initiated with the intention of supplementing more detailed studies done on an ESCA/Auger instrument at ERL and possibly develop a "finger-print" method that would permit the rapid identification of sample films. Also, the quantitative measurement capabilities of the microprobe could contribute to improved quantification in the ESCA/Auger analysis and in certain circumstances help identify potential models for the films under investigation.

Studies on corrosion in coal-water slurry pipelines and its inhibition by oxyanions such as molybdate, tungstate, chromate, phosphate and oxalate are currently being carried out in our laboratories by electrochemical and weight loss measurement techniques. Corrosion inhibition achieved by using oxyanions could be due to either interface or interphase protective films formed on the surface of the steel. In order to throw more light on the corrosion inhibition mechanism, these initial electron microprobe studies of the inhibitor films formed by the oxyanions on the steel samples were undertaken and the results obtained are reported in this paper.

EXPERIMENTAL

MATERIALS

The nominal composition of the steel AISI 1010 used in the present studies is given in Table 1.

Description of steel coupons exposed to various oxyanion inhibitor solutions along with the experimental conditions are given in Table 2.

MICROPROBE MEASUREMENTS

Samples of size ~4 mm x 10 mm were cut from the inhibitor treated steel coupons. Taking care not to touch the surface these pieces were carefully flattened using jeweller's pliers along the edges of the samples. The pieces were then mounted on a microprobe specimen holder with silver paint and identified by marking with a fine pointed scriber.

Both the test and blank samples were mounted side-by-side in the microprobe to permit subtraction of the background signal rather than by calculating it on the basis of readings taken either side of the peak. This procedure eliminates the effects of adjacent X-ray lines, sloping backgrounds and also avoids the repeated spectrometer movements entailed in the conventional technique.

The measurements were performed in a CAMEBAX-MICRO at an accelerating potential of 10 keV using an electron beam ~10 μm diameter. An accelerating potential of 10 keV is a compromise between low voltage which concentrates the X-ray generation towards the surface and a high voltage that gives high X-ray intensities. Counting times were generally 10 or 20 seconds, as necessary to achieve a significant count. This procedure was repeated on 5 or 10 different areas to obtain a good average value from the surface being measured, and proved to be satisfactory for all the inhibitor films, with the exception of ferrous oxalate, which showed extreme sensitivity to the incident electron beam. Even a large diameter, low current, continually moving beam was unable to prevent radiation damage of a ferrous oxalate film. Figures 1, 2 and 3 show the iron (Fe), oxygen (O) and carbon (C) signals as a function of exposure time as measured by a stationary, or moving beam. By extrapolation back to zero exposure time, reasonable values of the 'true' observed counting rates were obtained. For films that are stable under the electron beam, a much smaller beam size could be employed, in principle, to test the film uniformity at submicron resolution.

RESULTS AND DISCUSSION

The observed counting rates for various standards at 10 keV are given in Table 3; it should be noted that the beam current used was different for the various standards.

In acid mine water, corrosion inhibition is achieved by using sodium oxalate as an inhibitor. The mechanism of corrosion inhibition in this system consists of forming of ferric oxalate complex anion $[Fe(C_2O_4)_3^{3-}]$, which undergoes thermal and photochemical decomposition to yield ferrous oxalate. Ferrous oxalate is deposited on a steel sample protecting the steel from further corrosive attack. Microprobe data of the ferrous oxalate deposit on a steel sample along with those of commercially obtained ferrous oxalate and of a sample synthesized in the laboratory are given in Table 4. The observed counts for iron, carbon and oxygen from all three samples were nearly the same, showing the identity of the deposit on the steel sample to be the same (i.e.) ferrous oxalate. X-ray powder patterns of these samples confirmed that they were ferrous oxalate dihydrate. The microprobe data show that 'finger print' identification of ferrous oxalate deposits on steel samples is feasible.

Microprobe analysis of fairly thick deposits of ferrous oxalate on steel samples yielded the data given in Table 5. There is a fair agreement between the observed and calculated weight percentages of iron and oxygen. Disparity in the data for carbon is attributable to the radiation damage of the sample during the measurement, caused by the incident electron beam.

The corrected mass per unit area (g/cm^2) for some inhibitor systems is given in Table 6. In the case of oxalate the average ratio of carbon to oxygen in the films is nearly 1:2 which indicates the presence of C_2O_4 units in the film. The amount of phosphorus in the phosphate films is $\sim 2.0 \times 10^{-7} g/cm^2$ which amounts to several monolayers based on the calculation that a single monolayer of phosphate corresponds to $2 \times 10^{-8} g/cm^2$.

Quantitative data on the amounts of W, Mo and Cr present in the thin inhibitor films on the steel samples are presented in Table 7. Signals from Mo, O_2, W and O_2 in these samples as a function of position are depicted in Fig. 4 to 7. Figures 4 to 7 show that longer exposure time of the steel samples to molybdate and tungstate solutions give more pronounced signals. The results (Table 7) show that the amounts of the metal ion present in the films is in the order - Cr>W>Mo which is in agreement with the data obtained by ESCA and Auger techniques. Based on the calculation that close packed oxygen atoms cover $23 Å^2$ per three atoms, the amounts of tungstate and molybdate correspond to approximately a monolayer. On the other hand, chromium values indicate the presence of several monolayers in the inhibitor film.

CONCLUSIONS

The results given in this report show that the electron microprobe can be used to supplement surface analysis data in a useful manner, indicating both the spatial location and quantity of surface deposit.

ACKNOWLEDGEMENT

The authors would like to thank Mr. V. Chartrand for making the line drawings.

Table 1 - Composition of steel (wt %)

Constituent	AISI 1010
C	0.070
Mn	0.330
S	0.011
P	0.011
Si	0.010
Cu	0.130
Ni	0.036

Table 2: Description of steel coupons analyzed by electron microprobe

Sample number	Solution composition	pH	Potential (mv)	Duration of exposure (h)
1	Deaerated 0.01M Na_2MoO_4	8.5	-202	2
2	Aerated 0.01M Na_2MoO_4	8.5	-202	18
3	Deaerated 0.01M Na_2WO_4	8.5	-180	2
4	Aerated 0.01M Na_2WO_4	8.5	-168	2
5	Deaerated 0.01M K_2CrO_4	8.5	open circuit	2
6	Aerated 0.01M K_2CrO_4	8.5	-368	2
01	Aerated 0.01M $Na_2C_2O_4$	8.5	open circuit	2
02	Aerated 0.01M $Na_2C_2O_4$ at 200°F	8.5	open circuit	2
03	Deaerated 0.01M $Na_2C_2O_4$	8.5	open circuit	2
04	Deaerated 0.01M NaH_2PO_4	8.5	open circuit	2
05	Deaerated 0.01M NaH_2PO_4 at 200°F	8.5	open circuit	2
06	Deaerated 0.01M $NH_4Fe(SO_4)_2$ and 0.03 M $Na_2C_2O_4$	2.5	open circuit	2
07	Aerated 0.01M $NH_4Fe(SO_4)_2$ and 0.03 M $Na_2C_2O_4$	2.5	open circuit	2

Table 3: Observed counting rate on standards at 10 kv

Standard	X-ray line	counts/sec*
Fe	Fe - Kα	980
C	C - Kα	33,000
$Si(O_2)$	O - Kα	9,000
Na(Cl)	Cl - Kα	15,900
GaP	P - Kα	3,700
ZnS	S - Kα	4,000
W	W - Mα	8,650
Mo	Mo - Lα	2,550
Cr	Cr - Kα	2,400

*Beam current may vary from standard to standard

Table 4: Ferrous oxalate comparisons - 10 sec counts
- 10 kV accelerating potential

Specimen	Fe	Background	C	Background	O_2	Background
Standards	11 460	700	69 100	12 500	26 910	17 540
Blank Al	67		1 120			
C on Al	907		2 170			
#1*	2 575	25	4 671	300	23 200	90
#2*	2 540		4 747		25 250	
#3*	2 620		4 631		24 150	

*# 1 deposit on steel, #2 commercial, #3 PMRL made

Table 5: Massive ferrous oxalate - observed & predicted weight percentages

	Fe	O_2*	C
Observed	22.5	88.4	6.8
Predicted	25.3	98.0	12.5

*Relative to O_2 in SiO_2

Table 6: Corrected mass per unit area for various inhibitor systems g/cm^2

System	Specimen	Na	C	P*	O_2	S
Sodium oxalate	#1	-	1.7×10^{-7}	-	6.3×10^{-7}	
"	#2	-	8.4×10^{-8}	-	1.6×10^{-7}	
"	#3	1.4×10^{-8}	2.2×10^{-7}	-	6.9×10^{-7}	
Sodium di-hydrogen phosphate	#4	-	1.7×10^{-7}	2.2×10^{-7}	1.6×10^{-6}	-
"	#5	-	3.7×10^{-7}	1.4×10^{-7}	1.5×10^{-6}	
Sodium oxalate +	#6	1.4×10^{-8}	2.9×10^{-6}	-	2.4×10^{-5}	5.8×10^{-8}
Ammonium ferric	#7		3.7×10^{-5}			
sulphate	#7	0.95 x 10-8	-	3.4 x 10-5	1.1 x 10-7	

*1 monolayer of phosphate tetrahedra $\doteq 2 \times 10^{-8}$ g/cm^2

Table 7: Corrected mass per unit area for tungstate, molybdate and chromate inhibitors on 1010 steel

Inhibitor	Specimen	g/cm^2	$Å^2/gm$*
WO_4^{2-}	#3	1.07×10^{-7}	28
	#4	1.2×10^{-7}	25
MoO_4^{2-}	#1	7.5×10^{-8}	22
	#2	2.8×10^{-8}	58
	#2 with stain	3.2×10^{-8}	50
CrO_4^{2-}	#5	5.2×10^{-7}	1.7†
	#6	5.0×10^{-7}	1.7

*MO_4 tetrahedra would cover $23Å^2$

† Equivalent to many layers of "chromate" molecules

APPENDIX

In microprobe analysis it is assumed that the generated X-rays are proportional to the mass of material excited.

For a massive specimen, the X-ray generation volume is ~0.3 - 1.0 μm in radius, absorption will reduce the number observed by a factor ~1 - 0.8; for soft X-rays e.g. O-Kα, C-Kα, the factor will be much stronger ~0.3 or worse. Back scattered electrons will carry away some of the incident beam's energy in proportion to the mean atomic number of the target. Fluorescence may increase some X-ray intensites by factors ~1 - 1.25. Hence, the observed intensity will need some correction before it is attributed to given amounts of material. In the Packwood and Brown model for $\phi(\rho)$*, we can assume that the mass thickness of importance is equal to $\frac{1}{\alpha}$ gm, where α^2 is the exponent in the Gaussian term.

* see figures A1 and A2

$$\phi(\rho z) = \gamma_0 \exp(-\alpha^2 \rho z^2) \, (1 - q \exp(-\beta \rho z))$$

$$q = \frac{\gamma_0 - \phi_0}{\gamma_0}$$

The absorption and backscatter effects may be corrected by integrating $\phi(\rho z)$ thus

$$\text{observed} = \int_0^\infty \phi(\rho z) \exp(\chi \rho z) \, d\rho z$$

$\chi = \mu \operatorname{cosec} \theta$, μ the X-ray mass absorption coefficient and θ the X-ray take-off angle with respect to the specimen surface. The fluorescence term can similarly be calculated and, hence, the correction factor determined for X-ray generation in the solid.

A thin film on the surface of a specimen will need little or nothing by way of correction terms save only that it will be ϕ_0 times more effectively excited than the same film in space!

Details of the correction process can be found in any standard text on microprobe analysis; the theoretical basis for $\phi(\rho z)$ equation can be found in Packwood & Brown (1981) - Ref. (1)

REFERENCE

1. Packwood, R.H. and Brown, J.D. "A Gaussian expression to describe $\phi(\rho z)$ for quantitative electron probe microanalysis", X-ray Spectrometry vol 10, pp138-146, (1981).

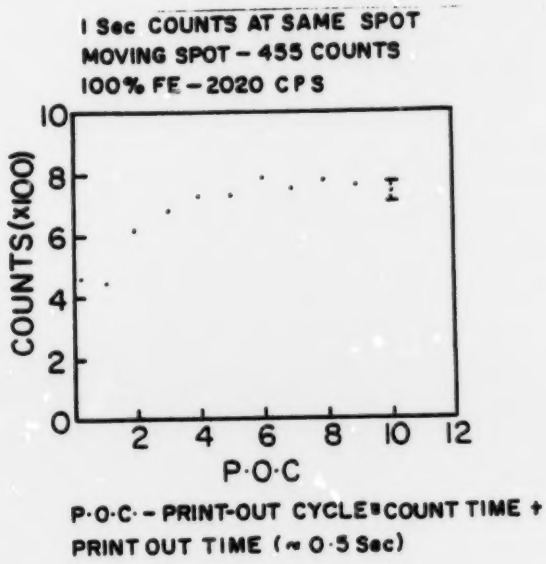
1 Sec COUNTS AT SAME SPOT
MOVING SPOT – 455 COUNTS
100% FE – 2020 CPS
COUNTS(x100)
P·O·C
P·O·C – PRINT-OUT CYCLE = COUNT TIME +
PRINT OUT TIME (≈ 0·5 Sec)

Fig. 1. Fe in oxalate. (neg 11349)

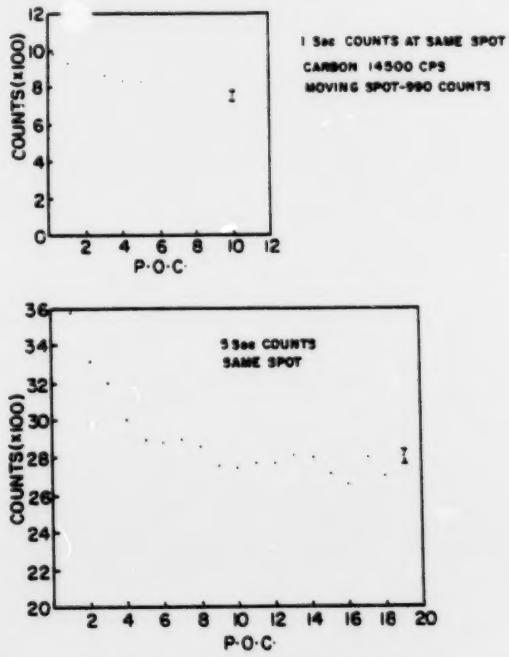

Fig. 2. Carbon in oxalate. (neg 11347)

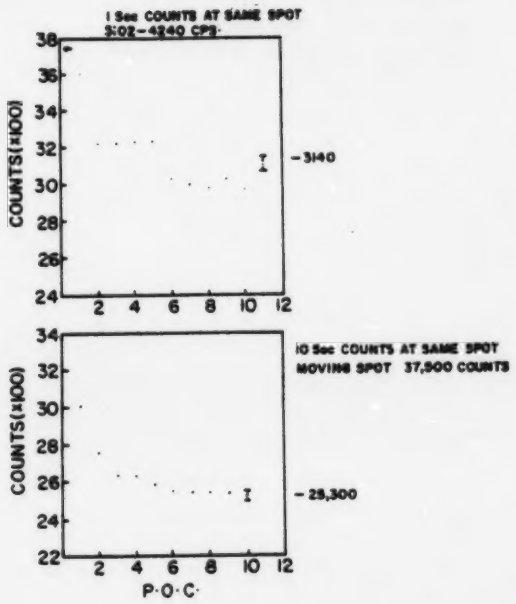

Fig. 3. Oxygen in oxalate. (neg 11348)

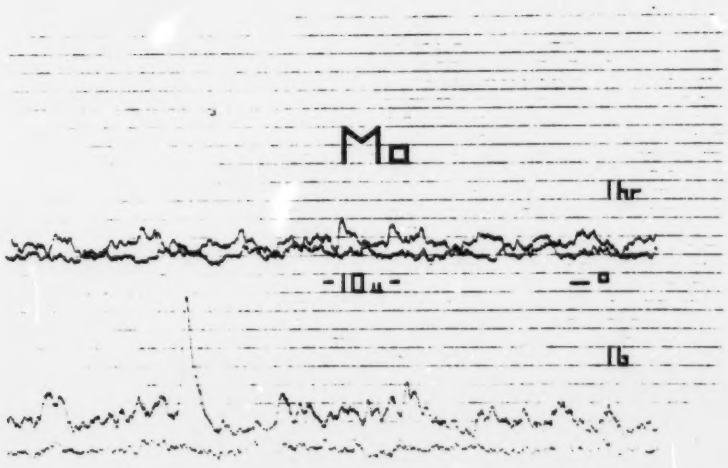

Fig. 4. Line trace for Mo in Molybdate film (10 kV).(neg 11350)

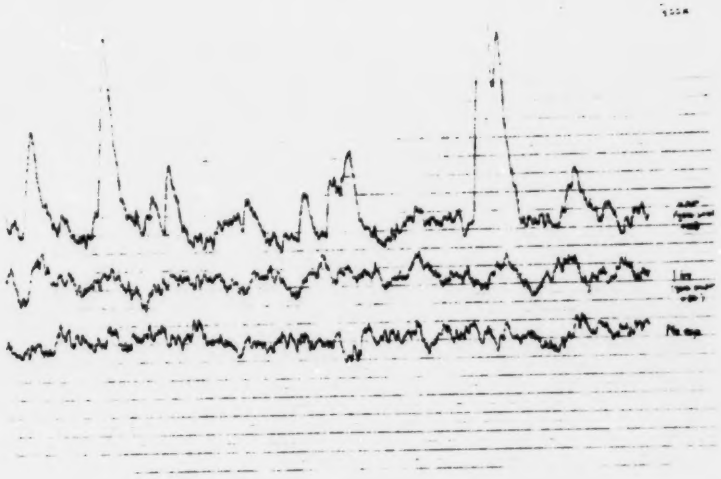

Fig. 5. Line trace for O_2 in molybdate film (10 kV). (neg 11352)

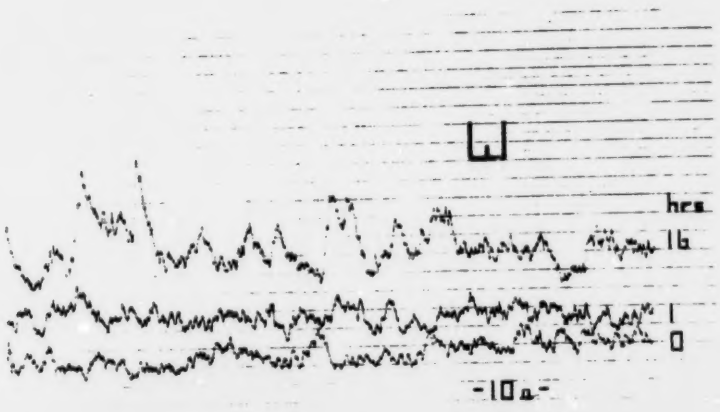

Fig. 6. Line trace for W in tungstate film (10 kV). (neg 11351)

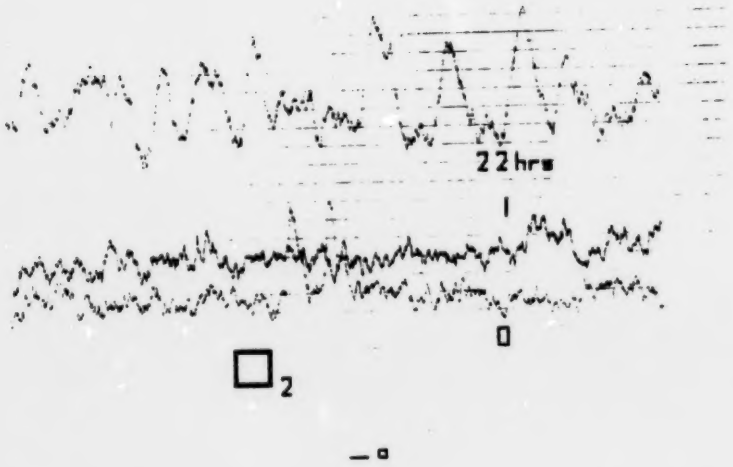

Fig. 7. Line trace for O_2 in tungstate film (10 kV). (neg 11345)

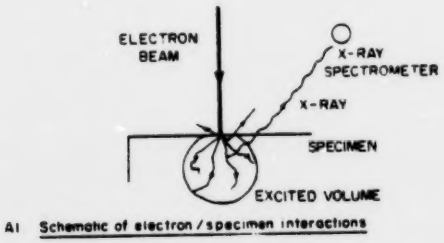

A1 Schematic of electron / specimen interactions

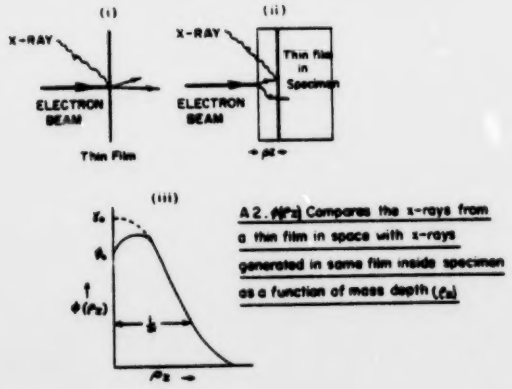

A2. Compares the x-rays from a thin film in space with x-rays generated in same film inside specimen as a function of mass depth

Fig. 8. (neg 11346)

POOR

QUALITY

ORIGINAL